CMS Physics Analysis Summary

Contact: cms-pag-conveners-bphysics@cern.ch 2013/11/28

Measurement of $\frac{\sigma(B_c^{\pm})\times \mathrm{Br}(B_c^{\pm}\to J\psi\pi^{\pm})}{\sigma(B^{\pm})\times \mathrm{Br}(B^{\pm}\to J\psi K^{\pm})}$ and $\frac{\mathrm{Br}(B_c^{\pm}\to J\psi\pi^{\pm}\pi^{\pm}\pi^{\mp})}{\mathrm{Br}(B_c^{\pm}\to J\psi\pi^{\pm})}$ at $\sqrt{s}$=7 TeV.

The CMS Collaboration

Abstract

The $B_c^{\pm} \to J/\psi\pi^{\pm}$ and $B_c^{\pm} \to J/\psi\pi^{\pm}\pi^{\pm}\pi^{\mp}$ decay modes are studied in CMS in the kinematic region where the transverse momentum of the $B_c^{\pm}$ meson is greater than 15 GeV/c and within the central rapidity region $|y| < 1.6$. Two ratios are measured: $\frac{\sigma(B_c^{\pm})\times \mathrm{Br}(B_c^{\pm}\to J/\psi\pi^{\pm})}{\sigma(B^{\pm})\times \mathrm{Br}(B^{\pm}\to J/\psi K^{\pm})} = (0.48 \pm 0.05\,(stat) \pm 0.04\,(syst)\,^{+0.05}_{-0.03}\,(\tau_{Bc})) \times 10^{-2}$ and $\frac{\mathrm{Br}(B_c^{\pm}\to J/\psi\pi^{\pm}\pi^{\pm}\pi^{\mp})}{\mathrm{Br}(B_c^{\pm}\to J/\psi\pi^{\pm})} = 2.43 \pm 0.76\,(stat)\,^{+0.46}_{-0.44}\,(syst)$.

1 Introduction

The $B_c^{\pm}$ meson is the ground state of $\bar{b}c$ ($b\bar{c}$) system. It carries two different heavy flavors, and thus represents a unique laboratory in which study heavy-quark dynamics. In the $B_c^{\pm}$ weak decays, both the c and b quarks compete through the spectator diagram. The annihilation process is also predicted to contribute to the final state at the level of 10% [1, 2]. The first $B_c^{\pm}$ experimental observations were performed by the CDF Collaboration in the semileptonic channel $B_c^{\pm} \to J/\psi l^{\pm}\nu$ [3]. The advent of the LHC has opened a new era for the $B_c^{\pm}$ investigation. A rich program of measurements is being carried out by LHCb at $2 < |\eta| < 5$; the complementary pseudorapidity region can be accessed by CMS. The CMS experiment, thanks to the excellent muon identification system and tracker detectors, allows, in particular, for the $B_c^{\pm} \to J/\psi\pi^{\pm}$ and $B_c^{\pm} \to J/\psi\pi^{\pm}\pi^{\pm}\pi^{\mp}$ final state studies. In this paper results of $\frac{\sigma(B_c^{\pm})\times \mathrm{Br}(B_c^{\pm}\to J/\psi\pi^{\pm})}{\sigma(B^{\pm})\times \mathrm{Br}(B^{\pm}\to J/\psi K^{\pm})}$ and $\frac{\mathrm{Br}(B_c^{\pm}\to J/\psi\pi^{\pm}\pi^{\pm}\pi^{\mp})}{\mathrm{Br}(B_c^{\pm}\to J/\psi\pi^{\pm})}$ are presented and discussed.

2 The CMS detector

The central feature of the Compact Muon Solenoid (CMS) apparatus is a superconducting solenoid of 6 m internal diameter, providing a field of 3.8 T. Within the field volume are a silicon pixel and strip tracker, a crystal electromagnetic calorimeter (ECAL) and a brass/scintillator hadron calorimeter (HCAL). Muons are measured in gas-ionization detectors embedded in the steel return yoke. Extensive forward calorimetry complements the coverage provided by the barrel and endcap detectors. The main sub-detectors used in this analysis are the silicon tracker and the muon systems. The inner tracker measures charged particles within the pseudorapidity range $|\eta| < 2.5$. The tracker is composed of layers totaling 66 million 100×150 μm^2 silicon pixels and 9.6 million silicon strips with pitch ranging from 80 to 183 μm immersed in a 3.8 T axial magnetic field, that provide precision tracking. Muons are measured in the pseudorapidity range $|\eta| < 2.4$, with detection planes made using three technologies: drift tubes, cathode strip chambers, and resistive plate chambers. Matching muons to tracks measured in the silicon tracker results in a transverse momentum resolution between 1 and 5%, for p_{T} values up to 1 TeV/c. The first level (L1) of the CMS trigger system, composed of custom hardware processors, uses information from the calorimeters and muon detectors to select the most interesting events in a fixed time interval of less than 4 μs. The High Level Trigger (HLT) processor farm further decreases the event rate from around 100 kHz to approximately 300 Hz, before data storage. The events used in the analysis reported here were collected with a trigger requiring the presence of a displaced dimuon system. A more detailed description of the CMS detector can be found in Ref. [4].

3 Event Selection

The analysis is based on the 2011 data sample collected by CMS at $\sqrt{s}$=7 TeV. Events selected with unprescaled displaced vertex dimuon triggers are considered, corresponding to an integrated luminosity of 5.1 fb^{-1}. The analysis is driven by the J/ψ meson reconstruction. The dimuon triggers apply topological and kinematic cuts on dimuon candidates: $\cos\alpha > 0.9$, where α is the pointing angle, in the transverse plane, between the dimuon momentum and the direction from the dimuon vertex to the mean pp collision position (beamspot); $L_{xy}/\sigma_{xy} > 3$, where L_{xy} is the transverse detachment between the dimuon vertex and the beamspot and σ_{xy} is the corresponding uncertainty; p_{T} ($\mu\mu$)>6.9 GeV/c. In addition, the two muon tracks must have opposite charges and are required to have a distance of closest approach of less than 0.5

cm. Selection requirements on the dimuon vertex probability (P_{VTX}) and p_T (μ) were made more severe as the luminosity increased and range from P_{VTX} >0.5% to P_{VTX} >15% and from p_T (μ)>0 to p_T (μ)>4 GeV/c, respectively. A cut on the muon pseudorapidity, $|\eta^{\mu}| < 2.2$, was included. The reconstructed J/ψ candidate is required to be consistent with that firing the trigger in a cone $\Delta R = \sqrt{(\Delta\eta)^2 + (\Delta\phi)^2} < 0.5$. The behavior of the trigger turn-on curves on the main variables (p_T, L_{xy}/σ_{xy}, cosα, confidence level of the J/ψ vertex) is studied both in data and MC to verify that data are well reproduced by the simulation. Trigger requirements have been tightened offline to $p_T(J/\psi) > 7.1$ GeV/c and $L_{xy}/\sigma_{xy} > 5$. $B_c^{\pm} \to J/\psi\pi^{\pm}$ ($B^{\pm} \to J/\psi K^{\pm}$) candidates are then formed combining the J/ψ meson with one track, assuming that it is a pion (kaon). The $B_c^{\pm} \to J/\psi\pi^{\pm}\pi^{\pm}\pi^{\mp}$ candidates are analogously formed combining the J/ψ meson with three tracks assuming that they are pions. The pion (kaon) candidates are required to have a track fit χ^2/ndof < 3, where ndof is the number of degrees of freedom; number of tracker hits > 6, number of pixel hits ≥ 2, $|\eta| < 2.4$ and $p_T > 0.9$ GeV/c. To save computing time the following cuts, inferred from MC simulation, are applied: the 3D impact parameter significance between each pion (kaon) and the J/ψ vertex is set less than 6; the ΔR between the J/ψ and the pion (kaon) track is required to be < 2.5 for $B_c^{\pm} \to J/\psi\pi^{\pm}$ ($B^{\pm} \to J/\psi K^{\pm}$). In the $B_c^{\pm} \to J/\psi\pi^{\pm}\pi^{\pm}\pi^{\mp}$ analysis, $\Delta R < 1$ is required for the highest p_T track, while $\Delta R < 1.6$ is required for the other two pions. The decay vertex is reconstructed using a kinematic vertex fit [5], which constrains the invariant mass of the two muons to the J/ψ nominal mass; the three (five) track vertex fit confidence level is required to be greater than 0.001. After the vertex fit, the track parameters are re-estimated at the fitted vertex, effectively using this vertex as a constraint. In case of multiple $B_c^{\pm}$ ($B^{\pm}$) candidates, the one with highest p_T is retained. Additional topological selections are required to improve the signal to noise ratio.

4 The $B_c^{\pm} \to J/\psi\pi^{\pm}\pi^{\pm}\pi^{\mp}$ signal

The search for $B_c^{\pm} \to J/\psi\pi^{\pm}\pi^{\pm}\pi^{\mp}$ decay is performed adding three-tracks, with total charge of ± 1, to the J/ψ candidate. The three pions are referred to as π_1, π_2 and π_3 from highest to lowest p_T. The selection cuts have been optimized maximizing the $S/\sqrt{(S+B)}$ figure of merit, where S is the signal yield obtained from a gaussian fit to the reconstructed truth-matched events of the MC sample[1], and B is the background inferred from data sidebands[2]. The optimized selection cuts are:

- $p_T(B_c) > 15$ GeV/c;
- $|y(B_c)| < 1.6$;
- B_c Vertex CL > 20 %;
- $cos\theta > 0.99$, where $cos\theta = L \cdot p_{B_c}/(|L||p_{B_c}|)$, θ being the angle between the candidate B_c momentum vector (p_{B_c}) and the detachment (L) between the decay vertex and the beamspot, evaluated in the plane transverse to the beam;
- $p_T(\pi_1) > 2.5$ GeV/c;
- $p_T(\pi_2) > 1.7$ GeV/c;
- $p_T(\pi_3) > 0.9$ GeV/c;
- $\Delta R(J/\psi, \pi_S) < 0.5$ where ΔR is taken from $\Delta\eta$ and $\Delta\phi$ derived from the J/ψ momentum vector and the sum of the momentum vectors of the three pions (π_S).

[1] i.e. events whose reconstructed tracks match those generated inside a cone of $\Delta R < 0.006$ for muons and $\Delta R < 0.01$ for hadrons.

[2] Sidebands are selected in the range [(m_{B_c}-8σ_{B_c}),(m_{B_c}-5σ_{B_c})] or [(m_{B_c}+5σ_{B_c}),(m_{B_c}+8σ_{B_c})], where m_{B_c} is the PDG mass for the B_c meson and σ_{B_c} is the width of the MC signal.

The resulting $B_c^{\pm} \to J/\psi\pi^{\pm}\pi^{\pm}\pi^{\mp}$ invariant mass distribution is shown in Fig. 1. The signal yield is 92 ± 27 events, its mass is 6.266 ± 0.006 GeV/c^2 (statistical error only) and its width is 0.021 ± 0.001 GeV/c^2, in agreement with the MC prediction. The B_c^+ MC sample has been produced using a dedicated generator (BCVEGPY)[6][7] interfaced with the PYTHIA hadronizer. The fit is performed through an unbinned maximum likelihood estimator; the signal is parametrized as a gaussian and the background as a second-order Chebyshev polynomial. A possible $B_c^{\pm} \to J/\psi K^{\pm}K^{\mp}\pi^{\pm}$ background contamination in the $B_c^{\pm} \to J/\psi\pi^{\pm}\pi^{\pm}\pi^{\mp}$ mode has been investigated and found to be negligible. The effect due to a missing π^0 has also been modeled. No significant variation of signal yield has been found.

5 The $B_c^{\pm} \to J/\psi\pi^{\pm}$ and $B^{\pm} \to J/\psi K^{\pm}$ signals

The figure of merit $S/\sqrt{(S+B)}$ has been optimized for the selection of the $B_c^{\pm} \to J/\psi\pi^{\pm}$ signal, in the same kinematic phase space defined for the $B_c^{\pm} \to J/\psi\pi^{\pm}\pi^{\pm}\pi^{\mp}$ decay (i.e. $p_T(B_c) > 15$ GeV/c and $|y(B_c)| < 1.6$). The procedure selects the following cut set:

- B_c Vertex CL > 6 %;
- $cos\theta > 0.9$;
- $p_T(\pi) > 2.7$ GeV/c;
- $\Delta R(J/\psi, \pi) < 1$.

The $B_c^{\pm} \to J/\psi\pi^{\pm}$ invariant mass distribution is shown in Fig. 2 (left). The $B^{\pm} \to J/\psi K^{\pm}$ signal is selected with the cut set optimized for the $B_c^{\pm} \to J/\psi\pi^{\pm}$ mode; it is shown in Fig. 2 (right). The $B_c^{\pm} \to J/\psi\pi^{\pm}$ and the $B^{\pm} \to J/\psi K^{\pm}$ invariant mass distributions are fitted through an unbinned maximum likelihood estimator. The $B_c^{\pm}$ signal is fitted with a gaussian and the background with a second-order Chebyshev polynomial. The signal yield is 176 ± 19, its mass 6.267 ± 0.003 GeV/c^2 (statistical error only), and its width, for this set of kinematic variables (y and p_T), 0.025 ± 0.003 GeV/c^2, consistent with the MC prediction. The effects due to a missing π^0 and to a possible reflection of the Cabibbo-suppressed $B_c^{\pm} \to J/\psi K^{\pm}$ mode in the $J/\psi\pi^{\pm}$ mass spectrum have also been modeled. No significant variation in both signal and background yield has been found. The $B^{\pm}$ invariant mass distribution is fitted with a double gaussian with a unique mean for the signal, and a second-order Chebyshev polynomial for the background. Additional contributions from partially reconstructed B^0 and $B^{\pm}$ decays are parametrized with functions inferred from inclusive $B^{\pm} \to J/\psi X$ and $B^0 \to J/\psi X$ MC samples.

6 The $\frac{\sigma(B_c^{\pm}) \times Br(B_c^{\pm} \to J/\psi\pi^{\pm})}{\sigma(B^{\pm}) \times Br(B^{\pm} \to J/\psi K^{\pm})}$ measurement

The ratio $\frac{\sigma(B_c^{\pm}) \times Br(B_c^{\pm} \to J/\psi\pi^{\pm})}{\sigma(B^{\pm}) \times Br(B^{\pm} \to J/\psi K^{\pm})}$ can be obtained through the relation

$$\frac{N(B_c^{\pm} \to J/\psi\pi^{\pm})}{N(B^{\pm} \to J/\psi K^{\pm})} = \frac{\sigma(B_c^{\pm}) \times Br(B_c^{\pm} \to J/\psi\pi^{\pm}) \times \epsilon_{B_c^{\pm}}}{\sigma(B^{\pm}) \times Br(B^{\pm} \to J/\psi K^{\pm}) \times \epsilon_{B^{\pm}}} \quad (1)$$

where N is the number of signal events, $\epsilon_{B(c)^{\pm}}$ is the overall analysis efficiency for the $B^{\pm}$ and $B_c^{\pm}$ reconstruction. The efficiency is evaluated as a function of the candidate transverse momentum on the corresponding MC samples; the B_c^+ meson production is simulated through the dedicated BCVEGPY generator, while that of $B^{\pm}$ is simulated using PYTHIA. The efficiency is computed in 24 transverse momentum bins for $B_c^{\pm}$ and 19 bins for $B^{\pm}$; the bin size is determined by the MC available statistics. The efficiency in the $i-th$ bin is evaluated as $\epsilon_i = \frac{N_i^{reco}}{N_i^{GEN}}$ where

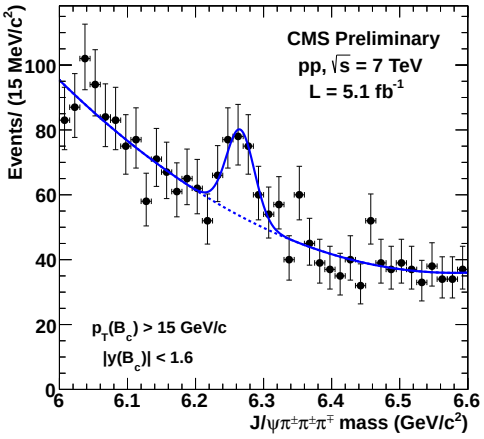

Figure 1: $J/\psi\pi^{\pm}\pi^{\pm}\pi^{\mp}$ invariant mass distribution.

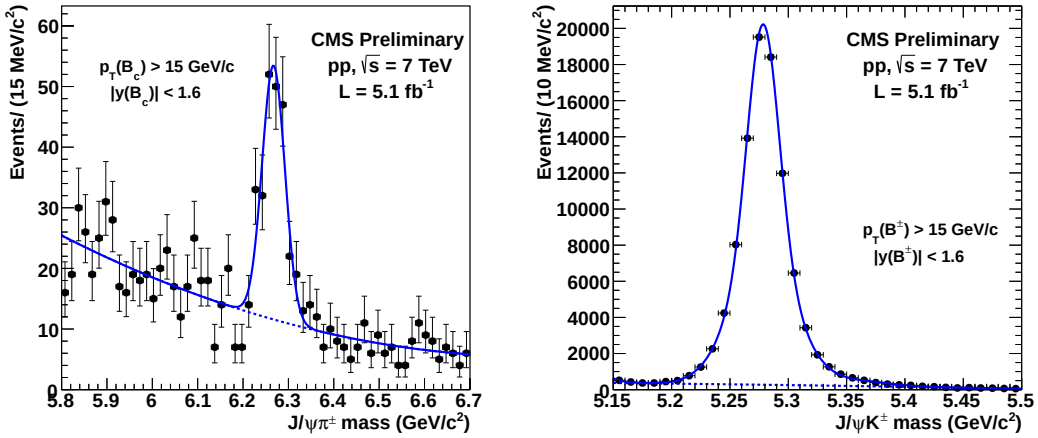

Figure 2: $J/\psi\pi^{\pm}$ invariant mass distribution (left) and $J/\psi K^{\pm}$ invariant mass distribution (right).

N_i^{reco} is the number of reconstructed and truth matched events in the given bin, and N_i^{GEN} is the number of generated $B_c^{\pm}$ ($B^{\pm}$) mesons in the same bin.
Data are corrected event-by-event according to their transverse momentum and the related MC efficiency. The efficiency-corrected mass plots for J/ψ $K^{\pm}$ and J/$\psi\pi^{\pm}$ are shown in Fig. 3. The efficiency corrected yields $Y_{Bc} = 6490 \pm 701$ and $Y_B = 1361156 \pm 5375$ are obtained by fitting the distributions shown in Fig. 3. The ratio measurement and its statistical uncertainty are:

$$\frac{\sigma(B_c^{\pm}) \times \mathrm{Br}(B_c^{\pm} \to J/\psi\pi^{\pm})}{\sigma(B^{\pm}) \times \mathrm{Br}(B^{\pm} \to J/\psi K^{\pm})} = (0.48 \pm 0.05) \times 10^{-2}. \quad (2)$$

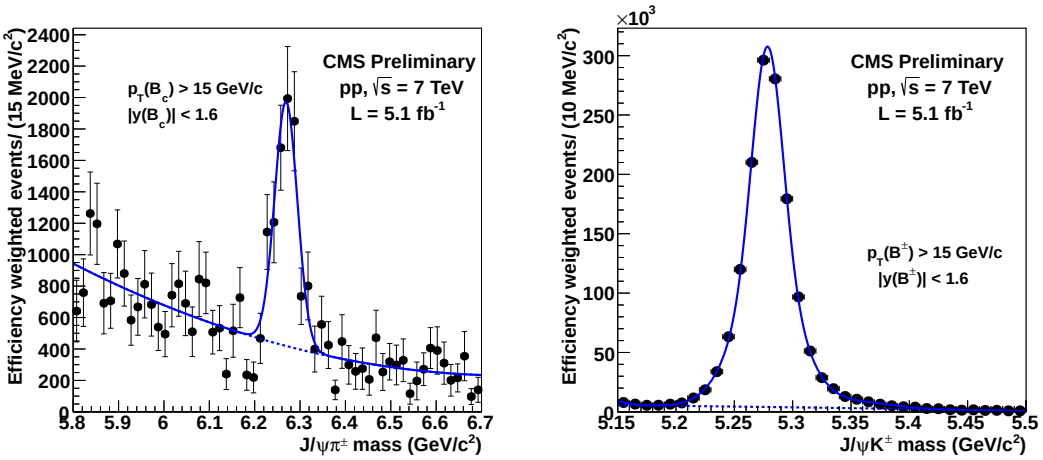

Figure 3: J/$\psi\pi^{\pm}$ (left) and J/$\psi K^{\pm}$ (right) efficiency-corrected mass distributions.

6.1 The $\frac{\sigma(B_c^\pm)\times Br(B_c^\pm\to J/\psi\pi^\pm)}{\sigma(B^\pm)\times Br(B^\pm\to J/\psi K^\pm)}$ systematic uncertainty

The global systematic error is estimated by adding in quadrature the different contributions listed in Table 1.

Syst. error	Percentage	Abs. value (10^{-2})
Split sample	0	0
Fit variant	5.6	0.03
MC finite size	2.2	0.01
Efficiency binning	4.1	0.02
Total uncertainty	7.3	0.04
B_c lifetime	$^{+10.9}_{-5.2}$	$^{+0.05}_{-0.03}$

Table 1: Systematic uncertainty contributions for the measurement of $\frac{\sigma(B_c^\pm)\times Br(B_c^\pm\to J/\psi\pi^\pm)}{\sigma(B^\pm)\times Br(B^\pm\to J/\psi K^\pm)}$.

The different sources of systematic uncertainty are:

- Split sample: data have been recorded with different trigger and pile-up conditions, following the increase of the LHC instantaneous luminosity. Statistical consistency has to be verified on the three independent sub-samples corresponding to the three different trigger periods, and on the two independent low and high pile-up sub-samples defined by the number of reconstructed primary vertices (PV): $1 \leq PV \leq 6$ and $PV \geq 7$ respectively. Since the sub-samples are statistically consistent, no systematic error from split sample is assigned.
- Fit variant: a possible systematic uncertainty due to the fitting technique is evaluated by varying the signal and background fit functions, and the range of the fitted distributions. In the $B_c^\pm \to J/\psi\pi^\pm$ a variant for the signal is represented by a double gaussian where the widths are fixed to the MC values, and for the background by different order Chebyshev polynomial (from 1^{st} to 3^{rd}) or by an exponential function. In the $B^\pm \to J/\psi K^\pm$ a variant for the signal is represented by a Crystal Ball function, and for the background by a different order Chebyshev polynomial (2^{nd} and 3^{rd} order). The structure due to the Cabibbo-suppressed contribution $B^\pm \to J/\psi\pi^\pm$ is parametrized with three different functions: a Crystal Ball, a Landau and a Gaussian form. The fit mass range is also varied. The fit variant systematic contribution is 5.6%.
- MC finite size: the efficiency is entirely derived from the simulation. The number of events in the simulation directly affects the accuracy of the efficiency determination. The efficiency uncertainty due to the MC finite size enters into the computation of Y_{B_c} and Y_B and is evaluated through pseudoexperiment studies. 1000 pseudoexperiment distributions are generated by randomly varying the efficiency value in each p_T bin within its error. Data are weighted with these efficiencies to calculate Y_{B_c} and Y_B. The resulting Y_{B_c} and Y_B yield distributions are fitted with a gaussian, whose width is taken as systematic uncertainty. The resulting systematic error is 2.2%.
- Efficiency binning: various bin values are tested for both the $B^\pm$ and $B_c^\pm$. A maximum deviation from the central value of the efficiency corrected yield Y_{B_c} (Y_B) of the order of 1.6% (3.8%) is found. It results in a deviation of 4.1% from the ratio value as in Eq. 6.
- $B_c^\pm$ lifetime: the available measurements of the $B_c^\pm$ lifetime are still affected by sizeable experimental uncertainty. The $B_c^\pm \to J/\psi\pi^\pm$ MC events are reweighted to cover

the lifetime world average $\tau_{B_c} = 0.452 \pm 0.032$ ps [8] and the efficiency is re-evaluated accordingly. The deviations in the ratio measurement ($+10.9\%$ and -5.2%) are taken as systematic uncertainties and are quoted separately in the results.

7 The $\frac{\mathbf{Br}(\mathbf{B_c^{\pm}} \to \mathbf{J/\psi \pi^{\pm}\pi^{\pm}\pi^{\mp}})}{\mathbf{Br}(\mathbf{B_c^{\pm}} \to \mathbf{J/\psi \pi^{\pm}})}$ measurement

The $B_c^{\pm} \to J/\psi\pi^{\pm}\pi^{\pm}\pi^{\mp}$ decay has been detected for the first time with a yield of about 100 events both in LHCb [9] and CMS [10]. Although some resonant substructures manifest in three and two-body invariant masses in both experiments, the quantitative determination of their contribution and mutual interferences in the five-body phase space would require a sophisticated amplitude analysis which is not feasible with the available statistics. However, the efficiency evaluation for the five-body decay of the $B_c^{\pm}$ could be affected by the decay dynamics and requires additional studies. Indeed, a visual inspection of the $\pi^{\pm}\pi^{\pm}\pi^{\mp}$ and $\pi^{\pm}\pi^{\mp}$ data mass projections reveals some hints of $a_1^{\pm}(1260)$ and $\rho^{\circ}(770)$ in the decay (Fig. 4).

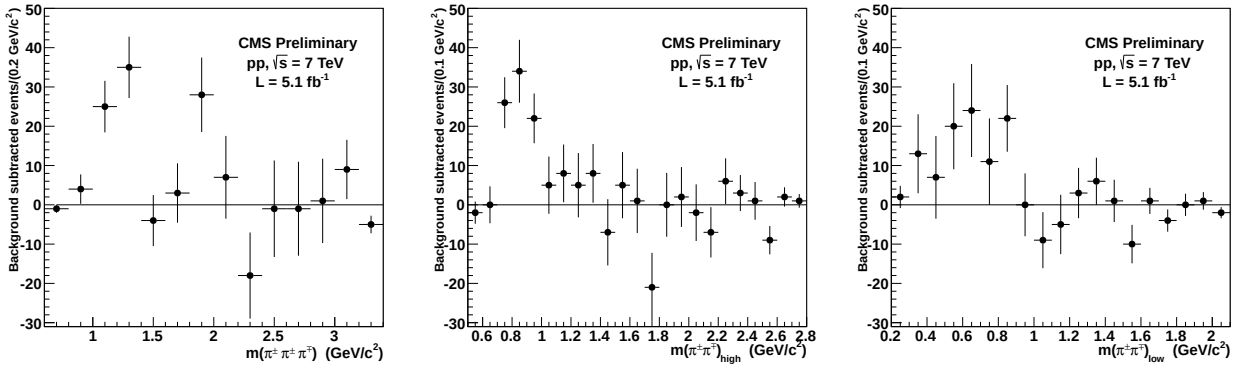

Figure 4: Background subtracted mass projection for $\pi^{\pm}\pi^{\pm}\pi^{\mp}$ (left), $(\pi^{\pm}\pi^{\mp})_{low}$ (center) and $(\pi^{\pm}\pi^{\mp})_{high}$. Since two same-sign pions are present in the final state, the two $\pi^{\pm}\pi^{\mp}$ pairs are identified as *low* and *high* according to their invariant mass.

A five-body decay of a spinless particle can be fully described in its center of mass by 8 independent mass-combinations of the type m_{ij} ($i \neq j$), where m_{ij} is the squared invariant mass of the pair of particles i and j in the final state (Dalitz plot representation). In the present case, the additional J/ψ mass constraint reduces to 7 the number of independent m_{ij}. The following seven mass-combinations have been chosen: $m^2(\mu^+\pi^+)_{low}$, $m^2(\pi^+\pi^-)_{high}$, $m^2(\mu^+\pi^-)$, $m^2(\pi^+\pi^+)$, $m^2(\mu^-\pi^+)_{low}$, $m^2(\mu^-\pi^+)_{high}$ and $m^2(\mu^-\pi^-)$; the *low* and *high* subscript refers to the lower and higher invariant mass combination where a π^+ is involved. The efficiency can be parametrized as a polynomial function of the type:

$$\epsilon = |p_0 + p_1 \cdot x + p_2 \cdot y + p_3 \cdot z + p_4 \cdot w + p_5 \cdot r + p_6 \cdot t + p_7 \cdot s| \tag{3}$$

where $x = m^2(\mu^+\pi^+)_{low}, y = m^2(\pi^+\pi^-)_{high}, z = m^2(\mu^+\pi^-), w = m^2(\pi^+\pi^+), r = m^2(\mu^-\pi^+)_{low}$, $t = m^2(\mu^-\pi^+)_{high}$, $s = m^2(\mu^-\pi^-)$ and p_i are the free parameters to be determined via an unbinned maximum likelihood fit on the generated events in the 7-th dimensional space through a binomial probability. The absolute value is required to protect the function from assuming negative values. The resulting efficiency function is used to weight the data event by event.

The efficiency-corrected data are fitted through an unbinned maximum likelihood estimator to extract the signal yield: $Y_{3\pi}$= 15765 $\pm$ 4627 (see Fig. 5). The result is

$$\frac{Br(B_c^{\pm} \to J/\psi\pi^{\pm}\pi^{\pm}\pi^{\mp})}{Br(B_c^{\pm} \to J/\psi\pi^{\pm})} = 2.43 \pm 0.76, \quad (4)$$

where the error is statistical only.

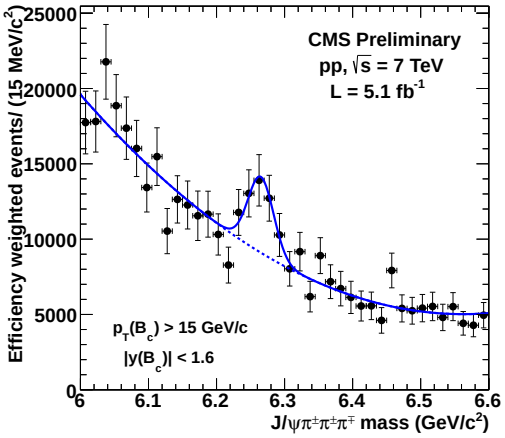

Figure 5: Fit to efficiency-corrected data for $B_c^{\pm} \to J/\psi\pi^{\pm}\pi^{\pm}\pi^{\mp}$.

7.1 The $\frac{Br(B_c^{\pm}\to J/\psi\pi^{\pm}\pi^{\pm}\pi^{\mp})}{Br(B_c^{\pm}\to J/\psi\pi^{\pm})}$ systematic uncertainty

The global systematic error is estimated by adding in quadrature the different contributions listed in Table 2.

Syst. error	Percentage	Abs. value
Split sample	7.4	0.18
Fit variant	10.7	0.26
MC finite size	4.1	0.10
Efficiency fit function	8.6	0.21
Efficiency binning	1.6	0.04
Tracking efficiency	7.8	0.19
Dimuon L_{xy}/σ_{xy} cut	+5	+0.13
Total uncertainty	$^{+19}_{-18}$	$^{+0.46}_{-0.44}$

Table 2: Systematic uncertainties for the measurement of $\frac{Br(B_c^{\pm}\to J/\psi\pi^{\pm}\pi^{\pm}\pi^{\mp})}{Br(B_c^{\pm}\to J/\psi\pi^{\pm})}$.

The different sources of systematic uncertainty are:

- Split sample: the limited statistics of the $B_c^{\pm} \to J/\psi\pi^{\pm}\pi^{\pm}\pi^{\mp}$ has not allowed for a trigger-period split-sample study. The statistics can be only split in low and high pile-up sub-samples according to the number of primary vertices. A systematics of 7.4% is evaluated.

- Fit variant: no variant with respect to a simple gaussian is allowed for the signal parametrization because of the limited statistics of the sample. Different order Chebyshev polynomials (from 1^{st} to 3^{rd}) are considered for the background description. Fits are also performed choosing various invariant mass ranges. The fit variant uncertainty is measured to be 10.7%.
- MC finite size: the finite size of the MC samples directly affects the accuracy of the efficiency determination. N efficiency curves are generated varying the parameters as sampled from a multivariate gaussian probability density function constructed from the fit covariance matrix. About 2000 pseudoexperiments are generated; the resulting $Y_{3\pi}$ distribution is fitted with a gaussian whose width is the efficiency corrected yield uncertainty. The systematic error on Y_{B_c} is evaluated as described in Sec.6.1. The systematic error on $Y_{3\pi}/Y_{B_c}$ is 4.1%.
- Efficiency fit function: the 7-dimensional efficiency in this analysis is parametrized with a polynomial function as described in Eq. 3. To check a possible systematics introduced by this form, data are weighted according to the binned efficiency distribution obtained from the MC samples. The efficiency is measured in six 4-GeV/c^2bins for each invariant mass and for each trigger path separately. The difference between the ratio measured using the binned efficiency distribution and the value quoted in Eq. 4 is taken as systematic uncertainty (8.6%).
- Efficiency binning: the maximum deviation from the central value of the efficiency corrected yield Y_{Bc} obtained by different choices of the efficiency binning (see Sec. 6.1) has been evaluated as systematic uncertainty and propagated to the ratio. It results in an error of 1.6%.
- Tracking efficiency: in this measurement two different multiplicity final states are compared. Assuming an efficiency tracking uncertainty for each pion track of 3.9% [11], a global 7.8% error has to be included in the final systematic evaluation.
- Dimuon L_{xy}/σ_{xy} cut: a value of +5% has been included in the systematics to account for the variation of the ratio with the dimuon L_{xy}/σ_{xy} cut.

8 Conclusions

The analysis of the $B_c^{\pm} \to J/\psi\pi^{\pm}$ and $B^{\pm} \to J/\psi K^{\pm}$ decays presented in this paper and based on the CMS 7 TeV data has permitted measurement of the ratio:

$$\frac{\sigma(B_c^{\pm}) \times \mathrm{Br}(B_c^{\pm} \to J/\psi\pi^{\pm})}{\sigma(B^{\pm}) \times \mathrm{Br}(B^{\pm} \to J/\psi K^{\pm})} = (0.48 \pm 0.05\,(stat) \pm 0.04\,(syst)\,^{+0.05}_{-0.03}\,(\tau_{B_c})) \times 10^{-2} \quad (5)$$

in a rapidity region complementary to that investigated by the LHCb collaboration [12].
The analysis of the $B_c^{\pm} \to J/\psi\pi^{\pm}\pi^{\pm}\pi^{\mp}$ decay mode has also permitted the determination of the ratio:

$$\frac{\mathrm{Br}(B_c^{\pm} \to J/\psi\pi^{\pm}\pi^{\pm}\pi^{\mp})}{\mathrm{Br}(B_c^{\pm} \to J/\psi\pi^{\pm})} = 2.43 \pm 0.76\,(stat)^{+0.46}_{-0.44}\,(syst) \quad (6)$$

which is in good agreement with the only other available estimate from the same LHCb experiment [9].

Acknowledgements

We congratulate our colleagues in the CERN accelerator departments for the excellent performance of the LHC and thank the technical and administrative staffs at CERN and at other CMS institutes for their contributions to the success of the CMS effort. In addition, we gratefully acknowledge the computing centres and personnel of the Worldwide LHC Computing Grid for delivering so effectively the computing infrastructure essential to our analyses. Finally, we acknowledge the enduring support for the construction and operation of the LHC and the CMS detector provided by the following funding agencies: BMWF and FWF (Austria); FNRS and FWO (Belgium); CNPq, CAPES, FAPERJ, and FAPESP (Brazil); MES (Bulgaria); CERN; CAS, MoST, and NSFC (China); COLCIENCIAS (Colombia); MSES (Croatia); RPF (Cyprus); MoER, SF0690030s09 and ERDF (Estonia); Academy of Finland, MEC, and HIP (Finland); CEA and CNRS/IN2P3 (France); BMBF, DFG, and HGF (Germany); GSRT (Greece); OTKA and NKTH (Hungary); DAE and DST (India); IPM (Iran); SFI (Ireland); INFN (Italy); NRF and WCU (Republic of Korea); LAS (Lithuania); CINVESTAV, CONACYT, SEP, and UASLP-FAI (Mexico); MBIE (New Zealand); PAEC (Pakistan); MSHE and NSC (Poland); FCT (Portugal); JINR (Dubna); MON, RosAtom, RAS and RFBR (Russia); MESTD (Serbia); SEIDI and CPAN (Spain); Swiss Funding Agencies (Switzerland); NSC (Taipei); ThEPCenter, IPST, STAR and NSTDA (Thailand); TUBITAK and TAEK (Turkey); NASU (Ukraine); STFC (United Kingdom); DOE and NSF (USA).

References

[1] I. Gouz et al., "Prospects for the B_c studies at LHCb", *Phys. Atom. Nucl* **67** (2004) 1559.

[2] H.-M. Choi and C.-R. Ji, "Non-leptonic two-body decays of the B_c meson in light-front quark model and the QCD factorization approach", *Phys. Rev. D* **80** (2009) 114003.

[3] CDF Collaboration, "Observation of the B_c meson in $p\bar{p}$ collisions at $\sqrt{s} = 1.8$ TeV", *Phys. Rev. Lett.* **81** (1998) 2432.

[4] CMS Collaboration, "The CMS experiment at the CERN LHC", *JINST* **3** (2008) S08004, doi:10.1088/1748-0221/3/08/S08004.

[5] G. Forden and D. Saxon, "Improving vertex position determination using a kinematic fit", *Nucl. Instrum. Meth. A* **248** (1986) 439, doi:10.1016/0168-9002(86)91031-4.

[6] C. Chang, C. Driouchi, P. Eerola, and X. Wu, "BCVEGPY: an event generator for hadronic production of the B_c meson", doi:10.1016/j.cpc.2004.02.005.

[7] J. Chang, C Wang and X. Wu, "BCVEGPY2.0: An upgraded version of the generator BCVEGPY with the addition of hadroproduction of the P-wave B_c states", doi:10.1016/j.cpc.2005.09.008.

[8] J. Beringer e al. (Particle Data Group), "Review of Particle Physics", *Phys. Rev. D* **86** (2012) and 2013 partial update for the 2014 edition (URL:http://pdg.lbl.gov).

[9] LHCb Collaboration, "First observation of the decay $B_c^{\pm} \to J/\psi\pi^{\pm}\pi^{\pm}\pi^{\mp}$", *Phys. Rev. Lett.* **108** (2012) 251802, doi:http://dx.doi.org/10.1103/PhysRevLett.108.251802.

[10] CMS Collaboration, "Observation of the decays $B_c^+ \to \mathrm{J}/\psi\ \pi^+$ and $B_c^+ \to \mathrm{J}/\psi\ \pi^+\pi^+\pi^-$ in pp collisions at $\sqrt{s} = 7$ TeV", *CMS Physics Analysis Summary* (2011).

[11] CMS Collaboration, "Measurement of Tracking Efficiency", CMS Physics Analysis Summary CMS-PAS-TRK-10-002, (2010).

[12] LHCb Collaboration, "Measurement of B_c^+ production and mass with the $B_c^+ \to J/\psi\pi^+$ decay", *Phys. Rev. Lett.* **109** (2012) 232001.